PAPER

Frequency Domain Adaptive Antenna Array for Broadband Single-Carrier Uplink Transmission

Wei PENG[†a)], ***Nonmember and*** **Fumiyuki ADACHI**[†], ***Fellow***

SUMMARY In this paper, a frequency domain adaptive antenna array (FDAAA) algorithm is proposed for broadband single-carrier uplink transmissions in a cellular system. By employing AAA weight control in the frequency domain, the FDAAA receiver is able to suppress the multi-user interference (MUI) and the co-channel interference (CCI). In addition, the channel frequency selectivity can be exploited to suppress the inter-symbol interference (ISI) and to obtain frequency diversity (or the multi-path diversity). Another advantage of the FDAAA algorithm is that its performance is not affected by the spread of angles of arrival (AOA) of the received multi-path signal. In this study the structure of FDAAA receiver is discussed and the frequency domain signal-to-interference-plus-noise-ratio (SINR) after weight control is investigated. The performance of the FDAAA algorithm is confirmed by simulation results. It is shown that, the optimal FDAAA weight to obtain the best BER performance is that which fully cancels the interference when single-cell system is considered; On the other hand, when multi-cell cellular system is considered, the optimal FDAAA weight depends on both the cellular structure and the target signal to noise ratio (SNR) of transmit power control (TPC).
key words: *frequency domain adaptive antenna array, single carrier transmission, uplink, cellular system*

1. Introduction

Broadband transmission is being used in the current wireless communication system and it is also going to be employed by the next generation system. Due to its multi-path fading with large delay spread, the broadband wireless channel is characterized by severe frequency selectivity [1]. As a result, it is necessary to suppress the inter-symbol interference (ISI). The ISI problem can be avoided by the use of multi-carrier transmission technique and the orthogonal frequency division multiple access (OFDMA) [2] has been proposed as a good solution for the downlink (from base station (BS) to mobile users) transmission. However, the multi-carrier transceivers are suffering from the high peak to average power ratio (PAPR) problem which can lead to severe performance degradation. To solve the high PAPR problem, the conventional single carrier (SC) transmission, again, attracted much interest. Actually, the ISI problem in the conventional SC transmission systems can be solved by introducing frequency domain equalization (FDE) [3] at the receiver. Recently, the combination of SC-FDE and frequency division multiple access (called SC-FDMA) [4] has been considered as a more suitable solution for the uplink (from mobile users to BS) transmission.

In a cellular system [5], the same carrier frequency may be reused by neighboring cells to increase the bandwidth efficiency. As a result, co-channel interference (CCI) [6] becomes the dominant performance limitation instead of the thermal noise. On the other hand, multi-user interference (MUI) [7] occurs when multiple users transmit simultaneously within the same cell. Therefore, interference cancelation at the BS is necessary in the uplink transmissions. It is reported in [8] that adaptive antenna array (AAA) can effectively suppress the interference in a frequency non-selective fading channel when the number of interferers is less than or equal to N_r, where N_r is the number of receive antennas.

In this paper, we will propose a combination of FDE and AAA, referred to as FDAAA, to combat both the ISI and CCI/MUI for the broadband SC uplink transmissions in a cellular system. In SC transmission, the AAA weight control can be applied to either the time domain or the frequency domain at the receiver. A joint time domain AAA and FDE algorithm has been proposed in [9]. Hereafter the time-domain algorithm is referred to as pre-fast Fourier transform (FFT) AAA algorithm. In the pre-FFT algorithm, the AAA weight control is performed before the FFT and the same AAA weight is used for all orthogonal frequencies. The limitation of this algorithm is that it is sensitive to the spread of angles of arrival (AOA) of the received multi-path signal. This limitation will be discussed later in Sect. 3. In our proposed FDAAA algorithm, the AAA weight control is performed on each frequency so that the performance will not be affected by the AOA distribution. Part of the results related to this study has been reported in [10].

The rest of the paper is organized as follows. The system model of SC uplink transmission in a cellular system will be described in Sect. 2. The FDAAA algorithm will be proposed in Sect. 3. Representative simulation results are shown in Sect. 4 and the paper will be concluded by Sect. 5.

2. System Model

The transmission in single cell case is considered at first and then extended to cellular case. The system model of uplink transmission is shown in Fig. 1. It is assumed that the BS is equipped with N_r receive antennas. The number of active users is U and each user has one transmit antenna. A block fading channel between each user and the BS is assumed, i.e., the channel remains unchanged during the transmission period of a block. In this paper, the symbol-spaced discrete

Manuscript received June 24, 2010.
Manuscript revised February 17, 2011.
[†]The authors are with the Dept. of Electrical and Communication Engineering, Graduate School of Engineering, Tohoku University, Sendai-shi, 980-8579 Japan.
a) E-mail: peng@mobile.ecei.tohoku.ac.jp
DOI: 10.1587/transcom.E94.B.2003

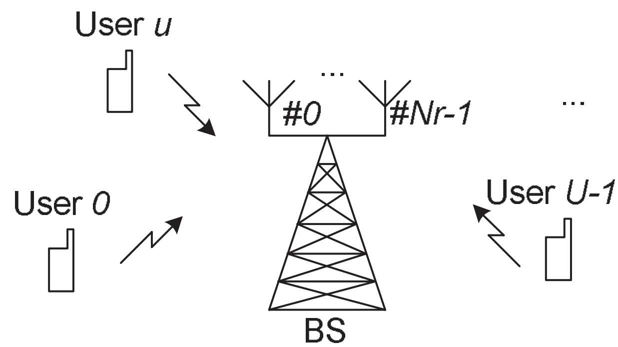

Fig. 1 Uplink transmission.

time representation of the signal is used. Assuming an L−path channel, the impulse response of the channel between user u and the mth antenna of the BS can be expressed as

$$h_{u,m}(\tau) = \sum_{l=0}^{L-1} h_{u,m,l}\delta(\tau - \tau_l), \tag{1}$$

where $h_{k,m,l}$ and τ_l are the path gain and time delay of the lth path, respectively. $h_{k,m,l}$ follows the complex Gaussian distribution (Rayleigh distribution) and satisfies $\sum_{l=0}^{L-1} E\{|h_{k,m,l}|^2\} = 1$ where $E\{\cdot\}$ represents the ensemble average operation. It is assumed that the time delay τ_l is a multiple integer of the symbol duration and $\tau_l = l$. The cyclic-prefixed block signal transmission is used to avoid inter block interference (IBI) and it is assumed that the cyclic prefix (CP) is longer than the maximum path delay of the signal. In the following, we omit the insertion and removal of the CP for the purpose of simplicity. The baseband equivalent received signal block $r_m(t); t = 0 \sim N_c - 1$ of N_c symbols at the mth antenna is given by

$$\begin{aligned} r_m(t) = &\sqrt{2P_0 d_0^{-\alpha} 10^{-\xi_0/10}} \sum_{l=0}^{L-1} h_{0,m,l} s_0(t-l) \\ &+ \sum_{u=1}^{U-1} \sqrt{2P_u d_u^{-\alpha} 10^{-\xi_u/10}} \sum_{l=0}^{L-1} h_{u,m,l} s_u(t-l) \\ &+ n_m(t) \end{aligned}, \tag{2}$$

where $s_u(t)$ and P_u are the transmit signal and transmit signal power of user $u(u = 0 \sim U - 1)$, respectively. Let the transmit signal from the $u = 0$th user be the desired signal, and the transmit signals from the other users be the interfering signals. d_0 represents the distance between the desired user and the BS; d_u represents the distance between the uth interfering user and the BS. α and ξ represent the path loss exponent and shadowing loss in dB, respectively. To simplify the analysis, $\xi = 0$ (no shadowing loss) is assumed. T is the symbol duration and $n_m(t)$ is the additive white Gaussian noise (AWGN).

The first term in the right-hand-side of (2) is the desired signal, the second term is the MUI signal and the last term is the noise signal. According to (2), the frequency domain representation of the received signal on the kth frequency is given by [11]

$$R_m(k) = H_{0,m}(k)S_0(k) + \sum_{u=1}^{U-1} H_{u,m}(k)S_u(k) + N_m(k), \tag{3}$$

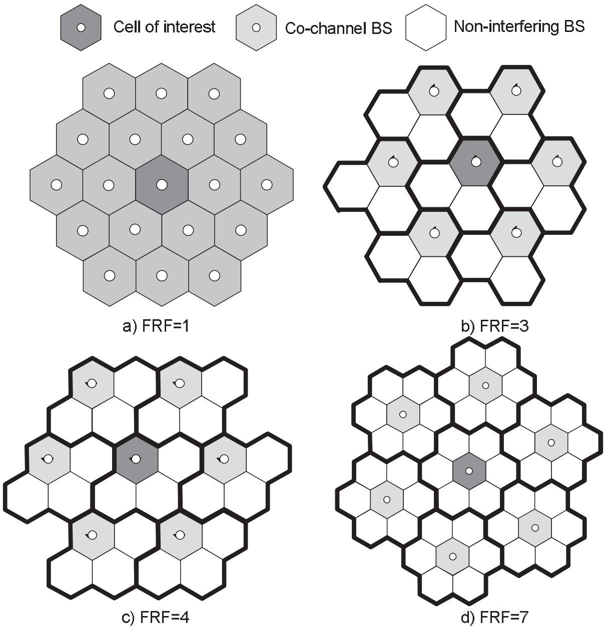

Fig. 2 Frequency reuse in cellular systems.

where

$$\begin{cases} S_u(k) = \sqrt{2P_u} \sum_{t=0}^{N_c-1} s_u(t) \exp\left(-j2\pi k \frac{t}{N_c}\right) \\ H_{u,m}(k) = \sum_{l=0}^{L-1} \sum_{t=0}^{N_c-1} h_{u,m,l} \exp\left(-j2\pi k \frac{t}{N_c}\right) \\ N_m(k) = \sum_{t=0}^{N_c-1} n_m(t) \exp\left(-j2\pi k \frac{t}{N_c}\right) \end{cases}. \tag{4}$$

The frequency domain received signal vector on the kth frequency $\mathbf{R}(k)$ is then expressed as

$$\mathbf{R}(k) = \mathbf{H}_0(k)S_0(k) + \mathbf{H}_u(k)S_u(k) + \mathbf{N}(k), \tag{5}$$

where $\mathbf{H}_u(k) = [H_{u,0}(k), H_{u,1}(k) \ldots H_{u,N_r-1}(k)]^T$ and $\mathbf{N}(k) = [N_0(k), N_1(k) \ldots N_{N_r-1}(k)]^T$ with the superscript ^{T} representing transpose operation.

In the cellular environment, there exists CCI from the neighboring cells due to the frequency reuse. The frequency reuse in cellular systems is shown in Fig. 2, where the frequency reuse factors (FRF) are 1, 3, 4 and 7, respectively. The commonly used first layer CCI model [6] is used here, i.e., only the CCI from the first layer neighboring cells will be considered and the number of CCI cells will be B=6.

The received signal at the mth antenna in (2) should be modified to include the CCI, and it can be rewritten as

$$\begin{aligned} r_m(t) = &\sqrt{2P_0 d_0^{-\alpha}} \sum_{l=0}^{L-1} h_{0,m,l} s_0(t-l) \\ &+ \sum_{u=1}^{U-1} \sqrt{2P_u d_u^{-\alpha}} \sum_{l=0}^{L-1} h_{u,m,l} s_u(t-l) \\ &+ \sum_{i=1}^{B} \sum_{u_i=0}^{U_i-1} \sqrt{2P_{i,u_i} d_{i,u_i}^{-\alpha}} \sum_{l=0}^{L-1} c_{i,u_i,m,l} s_{i,u_i}(t-l) \\ &+ n_m(t-l) \end{aligned}, \tag{6}$$

where s_{i,u_i} and P_{i,u_i} are respectively the transmit signal and transmit signal power of the u_ith user in the ith co-channel cell; d_{i,u_i} and $c_{i,u_i,m,l}$ are the distance and channel gain between the CCI user and the BS, respectively.

The frequency domain received signal on the kth frequency for (6) is given by

$$\begin{aligned} &R_m(k) \\ &= H_{0,m}(k) S_0(k) + \sum_{u=1}^{U-1} H_{u,m}(k) S_u(k), \\ &+ \sum_{i=1}^{B} \sum_{u_i=0}^{U_i-1} C_{i,u_i,m}(k) S_{i,u_i}(k) + N_m(k) \end{aligned} \tag{7}$$

where

$$\begin{cases} S_{u_i}(k) = \sqrt{2P_{i,u_i} d_{i,u_i}^{-\alpha}} \sum_{t=0}^{N_c-1} s_{u_i}(t) \exp\left(-j2\pi k \frac{t}{N_c}\right) \\ H_{u_i,m}(k) = \sum_{l=0}^{L-1} \sum_{t=0}^{N_c-1} c_{u_i,m,l} \exp\left(-j2\pi k \frac{t}{N_c}\right) \end{cases} \tag{8}$$

and the third term in the right-hand-side of (7) is the CCI component.

It is supposed that $N_r \geq U + U_1 + \ldots + U_B$ where U_i is the number of users in the ith co-channel cell. It is also supposed that the BS has the perfect knowledge of channel state information (CSI) between itself and all the users (including the desired user and the interfering users). Slow transmit power control (TPC) in each cell is assumed. The transmit power of each user in each cell is controlled so that the average signal-to-noise ratio (SNR) received at the corresponding BS will satisfy the system requirement on receive SNR, i.e.

$$\begin{cases} P_u/\sigma^2 = \Gamma_{TPC\_target} d_i^{\alpha} \\ P_{i,u_i}/\sigma^2 = \Gamma_{TPC\_target} d_{i,u}^{\alpha} \end{cases}, \tag{9}$$

where Γ_{TPC_target} is the TPC target SNR, σ^2 is the noise power and r_{i,u_i} is the distance between the CCI user and its own BS.

3. FDAAA Algorithm

In this section, the structure of the FDAAA algorithm will be discussed at first, then the FDAAA weight will be derived and the frequency domain signal to interference plus noise ratio (SINR) after weight control will be analyzed, and the tradeoff between the interference mitigation and diversity order of the FDAAA receiver will be discussed in the end.

3.1 Transmitter Structure

The transmitter structure is illustrated in Fig. 3(a) [12]. Binary data sequence is modulated and divided into a sequence of blocks of N_c data symbols. The last N_g symbols in each block are copied and inserted as the cyclic prefix into the guard interval (GI) and placed at the beginning of each block. In addition, pilot signals will be transmitted for channel estimation and AAA weight control. The frame structure

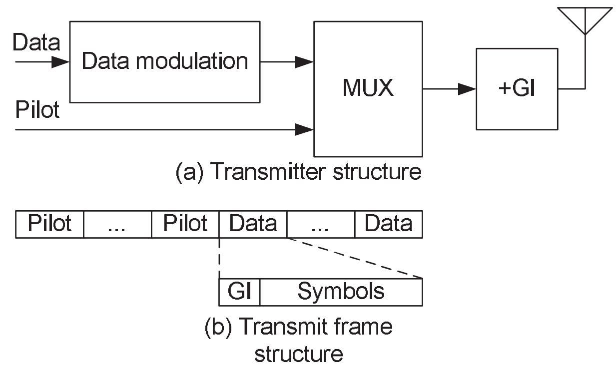

Fig. 3 Transmitter structure and transmit frame structure.

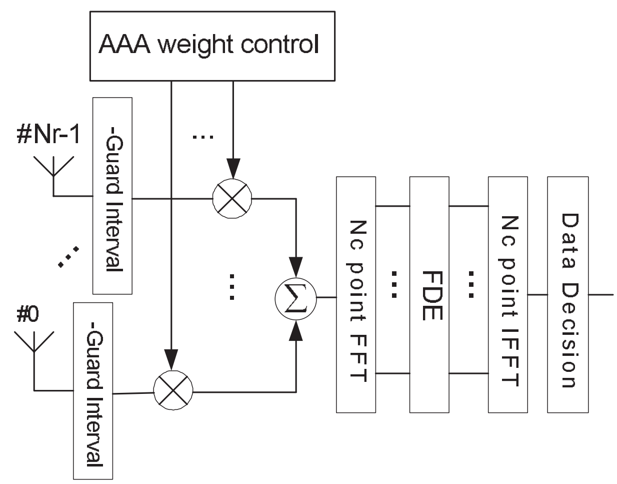

Fig. 4 Structure of pre-FFT AAA receiver.

of the transmit signal is shown in Fig. 3(b).

3.2 Receiver Structure

The transmit signal will be recovered from (6) at the receiver and the MUI and CCI components will be mitigated by using AAA weight control. We will describe the structure of pre-FFT AAA receiver at first and then propose the structure of FDAAA receiver.

3.2.1 Pre-FFT AAA Receiver

The pre-FFT AAA algorithm [9] performs AAA weight control in time domain, as shown in Fig. 4. Let $\mathbf{w}_{pre} = \left[w_{pre,0}, w_{pre,1} \ldots w_{pre,N_r-1}\right]$ represent the AAA weight control vector. The signal vector after the AAA combining can be written as

$$y(t) = \mathbf{w}_{pre}^T \mathbf{r}(t), \tag{10}$$

where $\mathbf{r}(t) = [r_0(t), r_1(t) \ldots r_{N_r-1}(t)]^T$ and $t = 0, 1 \ldots N_c - 1$. The AAA weight control vector can be obtained by using the normalized least mean square (NLMS) method [13]. With the aid of pilot sequence, the AAA weight control vector can be updated by

$$\begin{cases} \mathbf{w}'_{pre}(n) = \mathbf{w}'_{pre}(n-1) + 2\mu e(n) \frac{\mathbf{r}^*(n \bmod N_c)}{\|\mathbf{r}(n \bmod N_c)\|^2} \\ \mathbf{w}_{pre}(n) = \frac{\mathbf{w}'_{pre}(n)}{\|\mathbf{w}'_{pre}(n)\|} \end{cases}, \quad (11)$$

where $\|\cdot\|$ represents vector norm operation; $\mathbf{w}'_{pre}(n)$ $n = 1, 2, \cdots$ is an intermediate variable; and $e(n)$ is the error function defined as

$$\begin{aligned} e(n) = & \sum_{l=0}^{L-1} \sqrt{2P_0} \mathbf{w}^T_{pre}(n-1) \mathbf{h}_{0,l} s_0 (n \bmod N_c - l) \\ & - \mathbf{w}^T_{pre}(n-1) \mathbf{r}(n \bmod N_c) \end{aligned}. \quad (12)$$

The output of AAA combining $y(t)$ is then transformed to the frequency domain signal by N_c- point FFT transform, given by

$$Y(k) = \sum_{t=0}^{N_c-1} y(t) \exp\left(-j2\pi k \frac{t}{N_c}\right). \quad (13)$$

In the next, $Y(k)$ will be feed into the frequency domain equalizer and FDE will be performed so that

$$\tilde{Y}(k) = w_{FDE,k} \cdot Y(k). \quad (14)$$

The FDE weight $w_{FDE}(k)$ can be calculated following the minimum mean square error (MMSE) rule [14] given by

$$w_{FDE}(k) = \frac{\hat{H}_0^*(k)}{\left|\hat{H}_0(k)\right|^2 + (P_0/P_{NI})^{-1}}, \quad (15)$$

where the superscript * represents complex conjugate operation; P_{NI} is the power of interference plus noise; $\hat{H}_0^*(k)$ is the equivalent frequency domain channel gain after the AAA weight control, given by

$$\hat{H}_0(k) = \sum_{m=0}^{N_{r-1}} w_{pre,m} \sum_{l=0}^{L-1} \sum_{t=0}^{N_c-1} h_{0,m,l} \exp\left(-j2\pi k \frac{t}{N_c}\right). \quad (16)$$

The equalized frequency domain signal will then be transformed into the time domain by inverse FFT (IFFT) for data decision as

$$\tilde{d}(t) = \frac{1}{N_c} \sum_{k=0}^{N_c-1} \tilde{Y}(k) \exp\left(-j2\pi k \frac{t}{N_c}\right). \quad (17)$$

3.2.2 FDAAA Receiver

In the proposed FDAAA algorithm, AAA weight control is applied on each frequency. The structure of FDAAA receiver is shown in Fig. 5. Different from the OFDM system where each sub-carrier is modulated by different data-symbols, one data-symbol will be carried by all the frequencies in the single-carrier transmission. Therefore, instead of recovering the data-symbol on each sub-carrier, the data-symbol is recovered by using all the received frequency components after appropriately weighting them by the proposed method. Given the frequency domain received signal in (7), AAA weight control is performed as

$$\tilde{R}(k) = \mathbf{W}^T_{FDAAA}(k) \mathbf{R}(k), \quad (18)$$

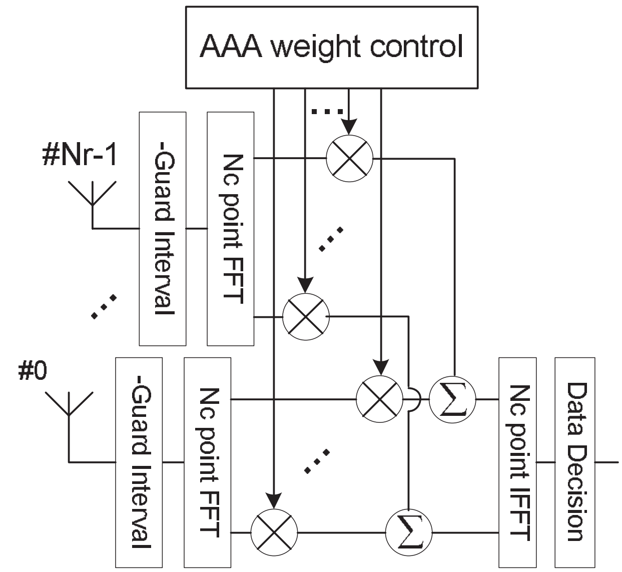

Fig. 5 Structure of FDAAA receiver.

where $\mathbf{W}_{FDAAA}(k) = [W_{FDAAA,0}(k) \cdots W_{FDAAA,N_r-1}(k)]^T$ is the FDAAA weight control vector. The FDAAA weight is designed to minimize the mean squared error (MSE) between the FDAAA output and the reference signal (the pilot sequence can be used as the reference signal). The MSE is given by

$$\begin{aligned} & E\left\{E^2(k)\right\} \\ & = E\begin{Bmatrix} \left[S_0(k) - \mathbf{W}^T_{FDAAA}(k)\mathbf{R}(k)\right]^* \\ \cdot\left[S_0(k) - \mathbf{W}^T_{FDAAA}(k)\mathbf{R}(k)\right] \end{Bmatrix} \\ & = E\begin{Bmatrix} S_0^*(k) S_0(k) - S_0^*(k) \mathbf{W}^T_{FDAAA}(k)\mathbf{R}(k) \\ -\mathbf{R}^*(k)\mathbf{W}^H_{FDAAA}(k) S_0(k) \\ +\mathbf{R}^*(k)\mathbf{W}^H_{FDAAA}(k)\mathbf{W}^T_{FDAAA}(k)\mathbf{R}(k) \end{Bmatrix} \end{aligned}, \quad (19)$$

where superscript ^{H} represents the conjugate transpose operation. To minimize the MSE in (19), the FDAAA weight $\mathbf{W}_{FDAAA}(k)$ must satisfy the following equality

$$\frac{\partial E\left\{E^2(k)\right\}}{\partial \mathbf{W}_{FDAAA}(k)} = 0. \quad (20)$$

By substituting (19) into (20), the following equality is obtained

$$E\begin{Bmatrix} -2S_0(k)\mathbf{R}^*(k) \\ +2\mathbf{R}^*(k)\mathbf{R}(k)\mathbf{W}_{FDAAA}(k) \end{Bmatrix} = 0. \quad (21)$$

By solving (21), the FDAAA weight vector $\mathbf{W}_{FDAAA}(k)$ is obtained by

$$\mathbf{W}_{FDAAA}(k) = \mathbf{C}^{-1}_{rr}(k)\mathbf{C}_{rd}(k), \quad (22)$$

where

$$\begin{aligned}&\mathbf{C}_{rr}(k)\\&=E\{\mathbf{R}^*(k)\mathbf{R}(k)\}\\&=\mathbf{A}_0^*(k)\mathbf{A}_0(k)+\sum_{u=1}^{U-1}\mathbf{A}_u^*(k)\mathbf{A}_u(k)\\&+\sum_{i=1}^{B}\sum_{u_i=0}^{U_i-1}\mathbf{A}_{i,u_i}^*(k)\mathbf{A}_{i,u_i}(k)+N_0\mathbf{I}\\&=\mathbf{A}_0^*(k)\mathbf{A}_0(k)+\mathbf{N}'(k)\end{aligned}\tag{23}$$

and

$$\mathbf{C}_{rd}(k)=E\{\mathbf{R}^*(k)S_0(k)\}=\mathbf{A}_0(k)S_0(k).\tag{24}$$

In (23), $\mathbf{A}_0(k)$ represents the propagation vector [8] of the transmit signal from the desired user, $\mathbf{A}_i(k)$ and $\mathbf{A}_{i,u_i}(k)$ are the propagation vector of the transmit signal form the MUI users and CCI users, respectively. It is assumed that the inference signals, the desired signal and the noise signal are uncorrelated with each other. N_0 represents the power spectrum of the AWGN (which is white in frequency domain) and $\mathbf{I}$ is an $N_r\times N_r$ standard matrix. $\mathbf{N}'(k)$ is used to represent the interference plus noise.

After performing the frequency domain AAA weight control, the time domain signal block estimate is obtained by N_c- point IFFT as

$$\hat{d}(t)=\frac{1}{N_c}\sum_{k=0}^{N_c-1}\hat{R}(k)\exp\left(-j2\pi k\frac{t}{N_c}\right)\tag{25}$$

for data decision.

3.3 Frequency Domain SINR Analysis

The SINR after the weight control on the kth frequency can be evaluated by [16]

$$\Gamma(k)=\frac{\mathbf{W}_{FDAAA}^*(k)\mathbf{R}_s(k)\mathbf{W}_{FDAAA}(k)}{\mathbf{W}_{FDAAA}^*(k)\mathbf{R}_{NI}(k)\mathbf{W}_{FDAAA}(k)},\tag{26}$$

where $\mathbf{R}_s(k)$ and $\mathbf{R}_{NI}(k)$ are the auto-correlation matrix of the received desired signal and the interference plus noise, respectively.

Property: if a matrix can be written as $\mathbf{Z}=\mathbf{T}^{-1}+\mathbf{P}\mathbf{Q}^{-1}\mathbf{P}^*$, then the inverse matrix of $\mathbf{Z}$ can be obtained by [17]

$$\mathbf{Z}^{-1}=\mathbf{T}-\mathbf{TP}(\mathbf{Q}+\mathbf{P}^*\mathbf{TP})^{-1}\mathbf{P}^*\mathbf{T}.\tag{27}$$

Let $\mathbf{Z}=\mathbf{C}_{rr}(k)$, $\mathbf{T}=\mathbf{R}_{NI}^{-1}(k)$, $\mathbf{P}=\mathbf{A}_0^*(k)$ and $\mathbf{Q}=\mathbf{I}$, then the inverse matrix $\mathbf{C}_{rr}^{-1}(k)$ can be calculated by substituting $\mathbf{Z}$, $\mathbf{T}$, $\mathbf{P}$ and $\mathbf{I}$ into (27).

$$\begin{aligned}&\mathbf{C}_{rr}^{-1}=\\&\mathbf{R}_{NI}^{-1}(k)-\mathbf{R}_{NI}^{-1}(k)\mathbf{A}_0^*(k)\\&\cdot\left[\mathbf{I}+\mathbf{A}_0(k)\mathbf{R}_{NI}^{-1}\mathbf{A}_0^*(k)\right]^{-1}\mathbf{A}_0(k)\mathbf{R}_{NI}^{-1}(k)\\&=\mathbf{R}_{NI}^{-1}(k)\left[\mathbf{I}-\frac{\mathbf{A}_0^*(k)\mathbf{A}_0(k)\mathbf{R}_{NI}^{-1}(k)}{\mathbf{I}+\mathbf{A}_0(k)\mathbf{R}_{NI}^{-1}\mathbf{A}_0^*(k)}\right]\\&=\left[\mathbf{I}+\mathbf{A}_0(k)\mathbf{R}_{NI}^{-1}\mathbf{A}_0^*(k)\right]^{-1}\mathbf{R}_{NI}^{-1}(k)\end{aligned}\tag{28}$$

The FDAAA weight is then obtained by substituting (24) and (28) into (22), given by

$$\begin{aligned}&\mathbf{W}_{FDAAA}(k)\\&=\left[\mathbf{I}+\mathbf{A}_0(k)\mathbf{R}_{NI}^{-1}\mathbf{A}_0^*(k)\right]^{-1}\mathbf{R}_{NI}^{-1}(k)\mathbf{A}_0(k)S_0(k)\end{aligned}\tag{29}$$

Finally, the SINR after the weight control can be obtained by substituting (29) into (26), as

$$\Gamma(k)=\mathbf{A}_0(k)\mathbf{R}_{NI}^{-1}(k)\mathbf{A}_0^*(k).\tag{30}$$

3.4 Discussion

The bit error rate (BER) performance of the detector using FDAAA algorithm is determined by two factors: the diversity order of the detector and the post processing SINR. As we know that the degree of freedom of the antenna array is limited by the number of antennas N_r. According to our assumption, $N_r\geq U+U_1+\cdots+U_B$ so that the FDAAA receiver has enough degree of freedom to deal with the MUI and the CCI. If all the interfering signals are treated as equivalent noise, the FDAAA detector will have full diversity order. However, the SINR given in (30) will be minimized. On the other hand, if the AAA weight is adjusted so that all the interference will be suppressed, then the diversity order will be minimized. And the SINR will be maximized. Therefore, there exists a tradeoff between the SINR level and the diversity order and it is interesting to find out how to perform interference cancelation so that the system performance can be optimized.

4. Simulation Results

In this section, the performance of the proposed FDAAA algorithm will be confirmed by simulation results. To focus on the proposed algorithm itself, no channel coding is used. In addition, $\xi=0$ (no shadowing loss) is assumed as already mentioned in Sect. 2. At first, single cell case is considered to study the performance of FDAAA receiver by assuming different AOA distributions. Then the performance of FDAAA receiver by using interference cancelation and full diversity is studied. Finally, the cellular system is considered. The performance of the FDAAA receiver assuming various diversity orders are studied and compared. The common parameters used in all the simulations are listed in Table 1, and the other parameters used in each simulation will be described later separately.

4.1 The Effect of AOA Spread

The objective of this simulation is to study the effect of AOA spread on the performance of FDAAA receiver and single cell case is considered. The propagation model is shown in Fig. 6. We assume three AOA distribution models and single cell case.

4.1.1 Non Spread AOA

Non spread AOA represents the situation that all the paths

Table 1 Simulation parameters.

Modulation	QPSK
Frame Length	256
Transmit Power Control	Slow TPC
Channel Model	*Frequency selective block Rayleigh fading*
Path loss exponent	3.5
Number of paths L	16
Power delay profile	Uniform
Received signal to noise ratio (SNR)	0 dB ∼ 20 dB
N_c	256

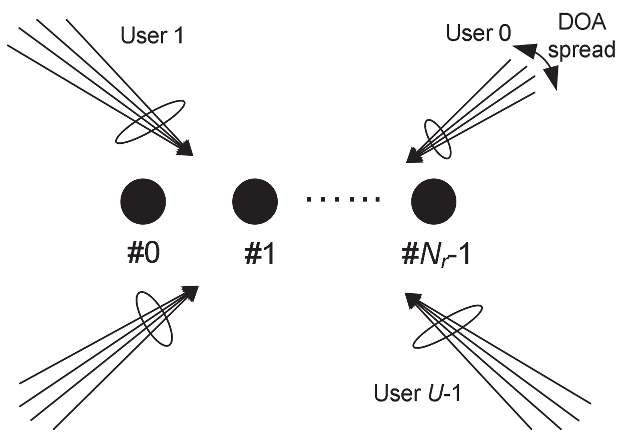

Fig. 6 Distribution of DOA spread.

associated with each user are coming from the same direction. And this assumption is used in [9]. Under this assumption, the AOA of the uth user can be represented by

$$\angle_{u,l} = \alpha_u; u = 0, \cdots, U-1; l = 0, \cdots, L-1, \quad (31)$$

where $\angle_{u,l}$ represents the AOA of the lth path of the uth user.

4.1.2 Uniform Distributed AOA

The AOA of L paths is assumed to be spread uniformly within the range of $2\Delta\alpha_u$, the probability density function (pdf) of the AOA of the uth user can be represented by

$$P(\angle_{u,l}) = \begin{cases} \frac{1}{2\Delta\alpha_u} & \alpha_u - \Delta\alpha_u \le \angle_{u,l} \le \alpha_u + \Delta\alpha_u \\ 0 & otherwise \end{cases}, \quad (32)$$

where $\Delta\alpha_u$ represents the range of AOA spread.

4.1.3 Gaussian Distributed AOA

In the Gaussian distribution model, the p.d.f. of the AOA of the uth user can be represented by

$$P(\angle_{u,l}) = \frac{1}{\sqrt{2\pi}\Delta\alpha_u} \exp\left(-\frac{(\angle_{u,l} - \alpha_u)^2}{2(\Delta\alpha_u)^2}\right), \quad (33)$$

where $\Delta\alpha_u$ represents the rms spread of AOA.

In the next, the performance of FDAAA receiver using the three AOA spread models will be studied. The performance of the pre-FFT AAA detection under exactly the same conditions will also be simulated to make comparison. To study the effects of different combinations of AOAs and different numbers of users/antannas (the number of users U is set equal to the number of receive antennas N_r), two-user case ($U = 2$) and four-user case ($U = 4$) are considered. For $U = 2$ case, the mean AOAs of the two users are set as 30° and 180°; and for $U = 4$ case, the mean AOAs of the four users are set as 30°, 140°, 220° and 270°. In both cases, the desired user's signal comes from a mean AOA of 30°. Non spread distribution, uniform distribution and Gaussian distribution models of AOA distribution are used and $\Delta\alpha_u$ for uniform distribution and Gaussian distribution varies between 4° and 8°. The AAA weight control vector to initialize the AAA weight calculation is $\mathbf{w}_{pre} = [1, 0, 0, 0]^T$ and the step size μ is 1/32 [9].

Non spread AOA distribution is used at first. The comparison between the average bit error rate (BER) performance of the FDAAA detection and the pre-FFT AAA detection is shown in Fig. 7(a). It can be observed that when there is no AOA spread, the FDAAA detection and the pre-FFT AAA detection achieve almost the same performance. Next, the effect of the uniform AOA distribution on the performance is shown in Fig. 7(b) for $\Delta\alpha_u$=4° and $\Delta\alpha_u$ = 8°. It can be observed that the performance of the FDAAA detection is exactly the same as the one without AOA spread. However, the performance of the pre-FFT AAA detection degrades significantly and error floor occurs even with the small α_u=4°. The Gaussian distributed AOA spread is considered in the next, the performance comparison between the FDAAA receiver and the pre-FFT AAA receiver is shown in Fig. 7(c). Similar results as the uniform distributed AOA are observed except that the performance degradation is less significant when the same α_u is used. The reason that the AOA spread degrades the performance of pre-FFT AAA detection is due to the fact that the interference suppression ability is limited by the number of antennas. By performing AAA weight control, only the interfering signals from $N_r - 1$ directions can be suppressed and the signals from the other directions remain as residual interference. However, when the AAA weight control is applied in frequency domain, its interference suppression ability is enough as long as the number of signal components on each frequency does not exceed the number of antennas.

4.2 Diversity Order/Interference Suppression in Single Cell Case

In this simulation, the performance of FDAAA receiver will be compared with the frequency domain receive diversity combining (FDRDC) receiver. The number N_r of receive antennas is chosen from N_r = 2, 3 and 4 and single cell case is considered.

Firstly, we consider the situation when no MUI exists. The performances of the two receivers are shown in Fig. 8(a). It is shown that when no MUI exists, the performance of the two receivers is almost the same as each other. As the number of antennas N_r increases, both FDAAA and

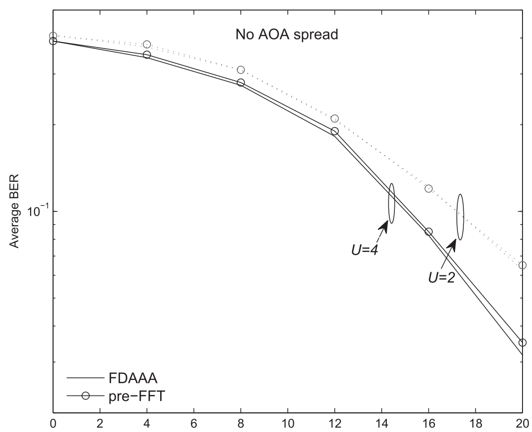

fig. 7(a) No AOA spread

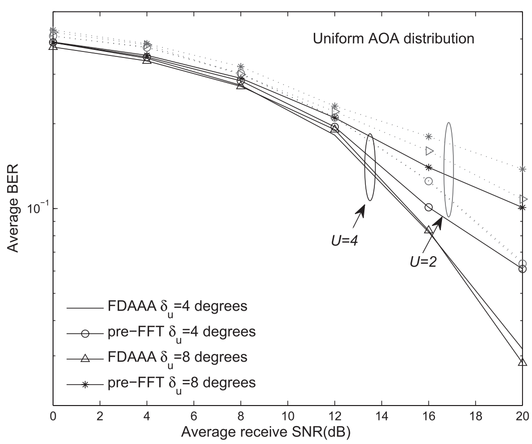

fig. 7(b) Uniform AOA distribution

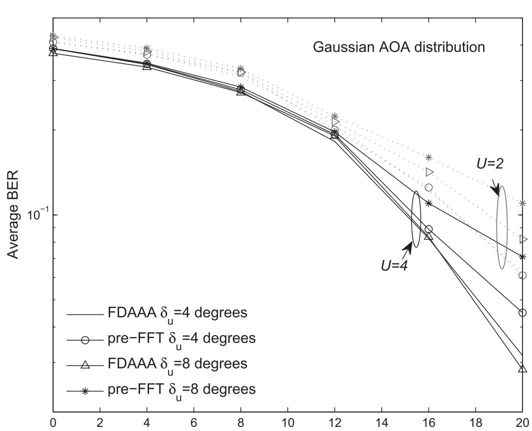

fig. 7(c) Gaussian AOA distribution

Fig. 7 Effect of AOA spread on pre-FFT AAA detection and FDAAA detection in single cell case.

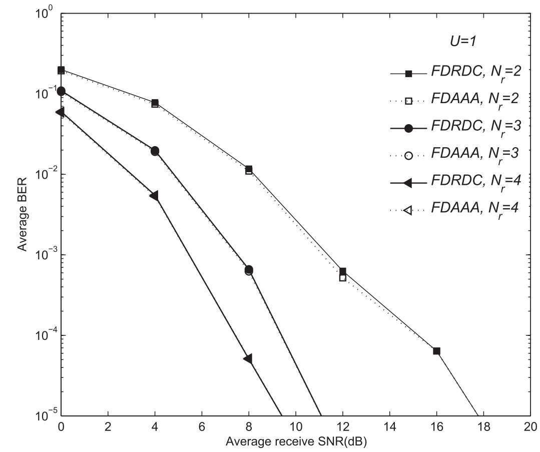

fig. 8(a)

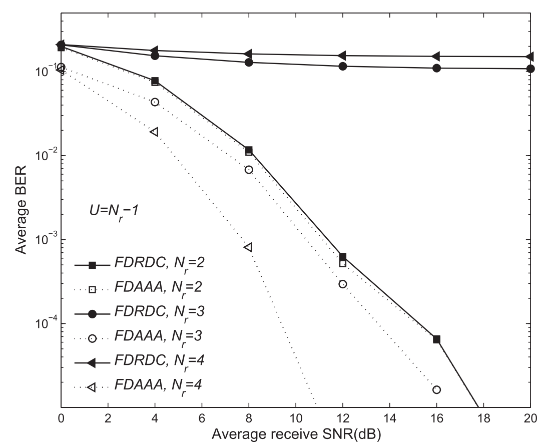

fig. 8(b)

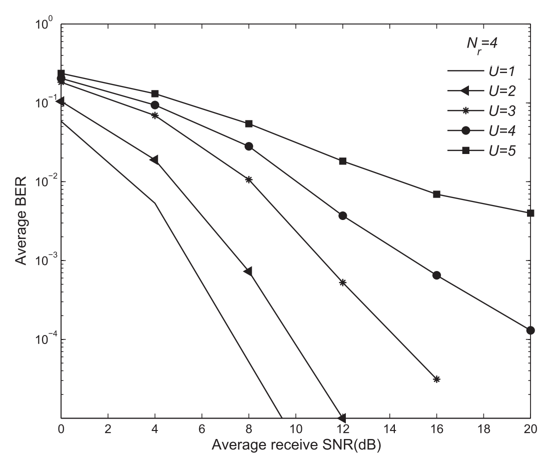

fig. 8(c)

Fig. 8 Diversity order/Interference suppression in single cell case.

FDRDC receivers benefit from the diversity gain and therefore, the BER performance improves. Next, we consider the situation when $U = N_r - 1$. In this simulation, the number of interfering users is 0, 1 and 2 for $N_r = 2, 3$ and 4 respectively. The performances of the two receivers are shown in Fig. 8(b). It is shown that with the existence of MUI, the performances of both modes degrade. The performance of FDRDC degrades and error floor occurs because that the residual MUI limits the performance. The performance of FDAAA degrades because of the reduction of diversity order. However, it is obvious that the performance degradation is much smaller with FDAAA than with FDRDC. The results show that when strong interference exists (in the single cell case, the MUI power can be as large as the desired signal), the interference suppression is more effective to improve the performance than the diversity order.

In the next, simulation is carried out to testify the performance of FDAAA versus the number of users U. The number of receive antennas N_r is set to 4 and U varies from 1 to 5. The performance is shown in Fig. 8(c). It is shown that given a fixed N_r, the performance becomes worse when U increases as we have discussed already. It is also shown that an error floor occurs when U exceeds N_r. This is due to the fact that AAA can and can only tolerate $N_r - 1$ interferers. Therefore, the number U of simultaneous users in the uplink transmission should be limited to $U \leq N_r$ when the FDAAA algorithm is applied.

4.3 Diversity Order/Interference Suppression in Cellular System

For the purpose of simplicity, 1 active user ($U = 1$) at each cell is assumed and the user is randomly located within the cell. Slow TPC is used to keep the average received signal SNR at each BS always at the target SNR for all users irrespective of the users' location. However, the interference powers from interfering users depend on their locations in the co-channel cells. In the following simulations, the performance of the FDAAA detection will be investigated by assuming cellular system. Cellular structures using FRF=1 and FRF=4 shown in Fig. 2(a) and Fig. 2(c) will be used. To find out the best way to perform interference suppression, It is assumed that the BS of interest has perfect CSI between itself and the desired user as well as the interfering CCI users and 7 working modes (Mode 0 ~ Mode 7) are defined in Table 2 for the FDAAA receiver. By using different working modes, the FDAAA receiver will suppress different number of CCI interferences while those interferences which are not canceled out will be treated as equivalent noise(Since perfect CSI at the BS of interest is assumed, the calculation of C_{rr} in (23) can be used to control the number of CCI to be suppressed. That is to say, if a CCI is to be suppressed, its CSI will be used to generate $A_u^*(k)A_u(k)$ in (23); while if the CCI is treated as equivalent noise, then its CSI will not be used and the CCI power will add to N_0 instead). The CCI level in Table 2 represents the number of remaining CCI interferences. For example, mode 0 has a diversity order of N_r which means that all the CCI interferences are treated as equivalent noise. Therefore, the corresponding CCI level is 6. In the simulations, if CCI suppression is performed, it will be performed on the CCI users with the most significant receive power at the BS.

Average BER performance of FDAAA receiver with 7 receive antennas (N_r=7) is studied at first. For the purpose of comparison, the maximum ratio combining (MRC) receiver with and without CCI is also simulated for FRF=1. In the following, the result of MRC receiver with CCI will be represented by MRC w/ CCI; and the result of MRC receiver without CCI will be represented by MRC w/o CCI. The simulation results are shown in Figs. 9(a) ~ (b) as a function of TPC target SNR which has been defined in (9). When FRF = 1, It is observed from Fig. 9(a) that: (1) In the region of low target SNR, Mode 0 achieves the best average BER performance. Therefore, when the performance is noise limited, the optimal way to achieve the best BER performance is to use all the degree of freedom as diversity. (2) As the target SNR increases, the optimal working mode corresponding to the best achievable BER performance changes by a order of Mode 0 → Mode 1 → · · · → Mode 5. It is shown that as the target SNR increases, the effect of CCI interference becomes more and more significant than that of the noise. As a result, interference suppression becomes more and more

Table 2 Working modes of FDAAA receiver.

Mode ♯	Diversity order	CCI level
0	N_r	6
1	$N_r - 1$	5
2	$N_r - 2$	4
3	$N_r - 3$	3
4	$N_r - 4$	2
5	$N_r - 5$	1
6	$N_r - 6$	0 (no CCI)

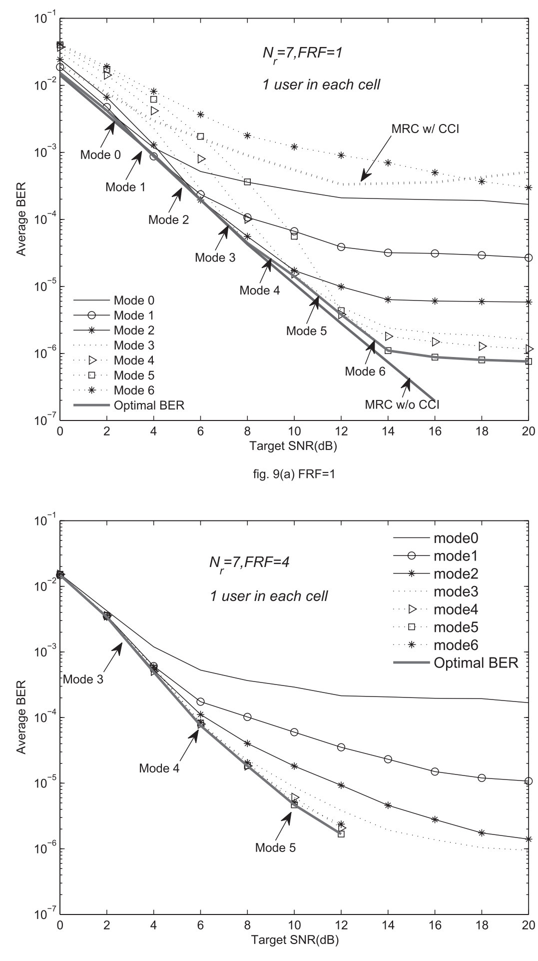

Fig. 9 Performance of FDAAA receiver with N_r=7 in cellular case.

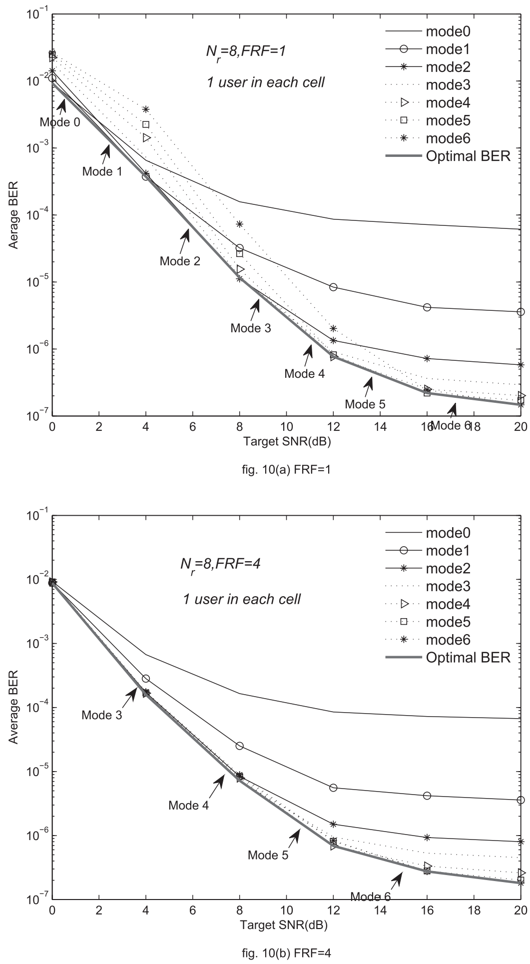

Fig. 10 Performance of FDAAA receiver with N_r=8 in cellular case.

powerful. (3) However, working Mode 6 does not achieve better performance than Mode 5 in high target SNR region. The reason is due to the incomplete interference suppression. Although the FDAAA receiver can minimize the average interference power, the instantaneous interference can not always be zero after the weight control. Therefore, the residual interference will limit the performance and cause the error floor. (4) When the BER performance of FDAAA is compared with MRC receiver, it can be observed that the best achievable performance of FDAAA receiver is almost the same as that of the MRC receiver without CCI. Therefore, it is verified that FDAAA can successfully suppress the CCI for single-carrier transmission in the cellular environment.

When FRF = 4, it can be observed that the best achievable BER performance is achieved by Mode 3, Mode 4 and Mode 5 in sequence as the target SNR increases.

The observations make it clear (A) the there exist a tradeoff between the interference suppression and the diversity order, as we have discussed in 3.4; (B) in addition, the best BER performance cannot be achieved by using one working mode. Instead, the optimal working mode that achieves the best performance vary when FRF changes or when the TPC target SNR changes.

If we increase the number of receive antennas N_r to 8, the receiver will have larger degree of freedom. The simulation results for N_r=8 are shown in Figs. 10(a) ∼ (b). It is observed that conclusions (A) and (B) are still true with N_r=8 case. In addition, it is interesting to note that Mode 6 achieves the best performance in the high target SNR region for both FRF=1 and FRF=4, which is different from the simulation results we observed from $N_r = 7$ case. Therefore, with the additional degree of freedom, FDAAA receiver can achieve the best BER performance by suppression of all the interference in the high SNR region.

5. Conclusions

In this paper, a single-carrier FDAAA algorithm has been proposed for the uplink detection in cellular systems. The proposed FDAAA receiver can deal with the interference while employ the frequency selectivity. The frequency domain SINR after the AAA weight control has been analyzed. It has been shown by the simulation results that the proposed FDAAA detection is not sensitive to the AOA spread and the receiver with N_r antennas can deal with up to $N_r - 1$ interferences. In addition, there exists a tradeoff between the interference suppression and diversity order. To find out the best way to use the degree of freedom of the FDAAA receiver, 7 working modes have been defined and their performance have been investigated. The simulation results have shown that the working mode to optimize the system performance depends on the FRF and the TPC target SNR as well.

References

[1] J.G. Proakis, Digital Communications, 4th ed., McGraw Hill, New York, 2001.

[2] R. Price and P.E. Green, “A communication technique for multipath channels,” IEEE Proc. IRE, vol.46, pp.555–570, March 1958.

[3] R. Van Nee and R. Prasad, OFDM for Wireless Multimedia Communications, Arctech House Publishers, UK, 1999.

[4] IEEE Standard 802. 11a-1999, IEEE standard for wireless LAN medium access control and physical layer specifications-Amendment I: High-speed physical layer in the 5 GHz band, Sept. 1999.

[5] S. Hara and R. Prasad, “Overview of multicarrier CDMA,” IEEE Commun. Mag., vol.35, pp.126–133, Dec. 1998.

[6] D. Falconer, S.L. Ariyavistakul, A. Benyamin-Seeyar, and B. Edison, “Frequency domain equalization for single-carrier broadband wireless systems,” IEEE Commun. Mag., vol.40, no.4, pp.58–66, April 2002.

[7] K. Sivanesan and N.C. Beaulieu, “Outage and BER of MRC diversity in band-limited micro-cellular systems with CCI,” IEEE Commun. Lett., vol.9, no.3, pp.207–209, March 2005.

[8] J.H. Winters, “Signal acquisition and tracking with adaptive arrays in the digital mobile radio system IS-54 with flat fading,” IEEE Trans. Veh. Technol., vol.42, no.4, pp.377–384, Nov. 1993.

[9] B.W. Kang, K. Takeda, and F. Adachi, “Performance of single-carrier frequency-domain adaptive antenna array,” Proc. IEEE VTC Fall 2007, pp.491–495, Baltimore, Sept. 2007.

[10] W. Peng and F. Adachi, “Frequency domain adaptive antenna array algorithm for single-carrier uplink transmission,” Proc. IEEE PIMRC 2009, pp.1–5, Tokyo, Sept. 2009.

[11] E.O. Brigham, The Fast Fourier Transform, Prentice-Hall, New York, 2002.
[12] F. Adachi, H. Tomeba, and K. Takeda, "Frequency-domain equalization for broadband single-carrier multiple access," IEICE Trans. Commun., vol.E92-B, no.5, pp.1441–1456, May 2009.
[13] Simon Haykin, Adaptive Filter Theory, Prentice Hall, New York, 2002.
[14] Monson H. Hayes Statistical Digital Signal Processing and Modeling, Wiley, 1996.
[15] M.A. Woodbury, Inverting Modified Matrices, Princeton, New Jersey, 1950.
[16] A.E. Zooghby, Smart Antenna Engineering, Arctech House, 2005.
[17] H.V. Henderson and S.R. Searle, "On deriving the inverse of a sum of matrices," SLAM Review, vol.23, no.1, pp.53–60, Jan. 1981.

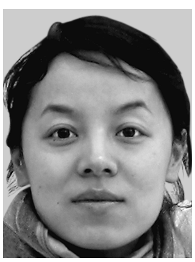

Wei Peng received her B.S. and M.S. degree in electrical engineering from Wuhan University, Wuhan, China, in 2000 and 2003 respectively. She received the Dr. Eng degree in electrical and electronic engineering from the University of Hong Kong, Hong Kong, in 2007. Since December 2007, she jointed Tohoku University and she is currently with the department of electrical and communication engineering as an assistant professor. Her research interests are in multiple antenna technology and cellular systems.

Fumiyuki Adachi received the B.S. and Dr. Eng degrees in electrical engineering from Tohoku University, Sendai, Japan, in 1973 and 1984, respectively. In April 1973, he joined the Electrical Communications Laboratories of Nippon Telegraph & Telephone Corporation (now NTT) and conducted various types of research related to digital cellular mobile communications. From July 1992 to December 1999, he was with NTT Mobile Communications Network, Inc. (now NTT DoCoMo, Inc.), where he lead a research group on wideband/broadband CDMA wireless access for IMT-2000 and beyond. Since January 2000, he has been with Tohoku University, Sendai, Japan, where he is a Professor of Electrical and Communication Engineering at the Graduate School of Engineering. His research interests are in CDMA wireless access techniques, equalization, transmit/receive antenna diversity, MIMO, adaptive transmission, and channel coding, with particular application to broadband wireless communications systems.